

A Dynamical Scaling Law for Jet Tomography

Carlos A. Salgado and Urs Achim Wiedemann
Theory Division, CERN, CH-1211 Geneva 23, Switzerland
(Dated: October 31, 2018)

Medium modifications of parton fragmentation provide a novel tomographic tool for the study of the hot and dense matter created in ultrarelativistic nucleus-nucleus collisions. Their quantitative analysis, however, is complicated by the strong dynamical expansion of the collision region. Here, we establish for the multiple scattering induced gluon radiation spectrum a scaling law which relates medium effects in a collision of arbitrary dynamical expansion to that in an equivalent static scenario. Based on this scaling, we calculate for typical kinematical values of the RHIC and LHC heavy ion programs medium-modified parton fragmentation functions for heavy ion collisions with realistic dynamical expansion.

For the study of the shortlived state of hot and dense matter produced in nucleus-nucleus collisions, novel tools become available at collider energies. In particular, the abundant production of high- p_\perp partons in hard processes dominates the high- p_\perp tails of hadronic particle spectra. These partons propagate through the medium while fragmenting into hadrons. Basic properties of the hot and dense matter such as the average in-medium pathlength of hard partons and the transverse colour field strength (energy density) they experience are thus reflected in the medium-dependence of parton fragmentation.

Motivated by this idea [1], several groups [2, 3, 4, 5] calculated in recent years gluon radiation spectra due to medium-induced multiple scattering contributions in order to understand the medium-dependence of hadronic cross sections. The aim of this letter is to extend previous studies [6, 7] to the full gluon radiation spectrum in a strongly expanding medium of small finite size, to calculate for the first time the medium-dependent fragmentation functions resulting from many soft interactions of the hard parton with the medium, and to explore observable consequences for collider experiments at RHIC and LHC.

Hadronic cross sections for high p_\perp particle production are calculated by convoluting the parton distributions of the incoming projectiles with the product $d\sigma^h(z, Q^2)$ of a perturbatively calculable partonic cross section σ^q and the fragmentation function $D_{h/q}(x, Q^2)$ of the produced parton, $d\sigma^h(z, Q^2) = \left(\frac{d\sigma^q}{dy}\right) dy D_{h/q}(x, Q^2) dx$. Here, $x = E_h/E_q$, $y = E_q/Q$ and $z = E_h/Q$ denote fractions between the virtuality of the hard process Q , and the energies of the produced parton and resulting hadron. If the produced parton loses with probability $P(\epsilon)$ an additional fraction $\epsilon = \frac{\Delta E}{E_q}$ of its energy due to medium-induced radiation, then the hadronic cross section is given in terms of the medium-modified fragmentation function [8, 9]

$$D_{h/q}^{(\text{med})}(x, Q^2) = \int_0^1 d\epsilon P(\epsilon) \frac{1}{1-\epsilon} D_{h/q}\left(\frac{x}{1-\epsilon}, Q^2\right). \quad (1)$$

The probability that a hard parton loses ΔE of its initial energy due to the independent emission of an arbitrary number of n gluons is determined by the medium-induced gluon energy spectrum $\frac{dI}{d\omega}$, [10]

$$P(\Delta E) = \sum_{n=0}^{\infty} \frac{1}{n!} \left[\prod_{i=1}^n \int d\omega_i \frac{dI(\omega_i)}{d\omega} \right] \times \delta \left(\Delta E - \sum_{i=1}^n \omega_i \right) \exp \left[- \int d\omega \frac{dI}{d\omega} \right]. \quad (2)$$

We evaluate the quenching weight (2) via its Mellin transform (see [10] for details), starting from the medium-induced BDMPS-Z gluon radiation spectrum [4, 11],

$$\omega \frac{dI}{d\omega} = \frac{\alpha_s C_F}{(2\pi)^2 \omega^2} 2\text{Re} \int_{\xi_0}^{\infty} dy_l \int_{y_l}^{\infty} d\bar{y}_l \int d^2\mathbf{u} d^2\mathbf{k} e^{-i\mathbf{k}_\perp \cdot \mathbf{u}} \times e^{-\frac{1}{2} \int_{\bar{y}_l}^{\infty} d\xi n(\xi) \sigma(\mathbf{u})} \frac{\partial}{\partial \mathbf{y}} \cdot \frac{\partial}{\partial \mathbf{u}} \mathcal{K}(\mathbf{y} = 0, y_l; \mathbf{u}, \bar{y}_l | \omega), \quad (3)$$

where

$$\mathcal{K} = \int \mathcal{D}\mathbf{r} \exp \left[i \int_{y_l}^{\bar{y}_l} d\xi \frac{\omega}{2} \left(\dot{\mathbf{r}}^2 - \frac{n(\xi) \sigma(\mathbf{r})}{i\omega} \right) \right]. \quad (4)$$

Medium properties enter $dI/d\omega$ via the product of the medium density $n(\xi)$ of scattering centers times the relative strength of the single elastic scattering cross section $\propto |a_0(\mathbf{q}_\perp)|^2$ measured by the dipole cross section $\sigma(\mathbf{r}) = 2C_A \int \frac{d\mathbf{q}_\perp}{(2\pi)^2} |a_0(\mathbf{q}_\perp)|^2 (1 - e^{-i\mathbf{q}_\perp \cdot \mathbf{r}})$. We consider the effect of arbitrarily many soft momentum transfers to the parton, when the path integral in (3) can be evaluated in the saddle point approximation [3, 4], $\sigma(\mathbf{r}) \approx C \mathbf{r}^2$. This is complementary to studies which consider one additional medium-induced gluon exchange via twist-4 matrix elements [12, 13], or up to $N \leq 3$ medium-induced momentum transfers in an opacity expansion [4, 5] of (3).

For the case of a nuclear medium without dynamical evolution, $n(\xi) = n_0$, the radiation spectrum (3) depends on the partonic in-medium pathlength L and the transport coefficient $n_0 C$. The latter measures the squared average momentum picked up by the partonic

projectile per unit pathlength [11]. Phenomenological estimates [2, 11, 14] range typically between $n_0 C = (50 \text{ MeV})^2/\text{fm}$ for normal nuclear matter and $n_0 C = (500 \text{ MeV})^2/\text{fm}$ for a hot quark-gluon plasma. Writing all energies in units of the characteristic gluon frequency $\omega_c = 2 n_0 C L^2$, the probability $P(\Delta E/\omega_c)$ depends on only one further, dimensionless parameter combination

$$R = n_0 C L^3. \quad (5)$$

We refer to R as “density parameter” since it characterizes the initially produced gluon rapidity density (see eq. (11) below).

Fig. 1 shows the quenching weights $P(\Delta E/\omega_c)$ calculated for a static nuclear medium and varying density parameters R . In comparison to earlier studies [10], we observe as a novel feature the occurrence of a discrete contribution p_0 in

$$P(\Delta E/\omega_c) = p_0 \delta(\Delta E/\omega_c) + p(\Delta E/\omega_c). \quad (6)$$

This is a consequence of considering a medium of realistic small size and opacity, where the projectile escapes the collision region with finite probability p_0 without further interaction. With increasing density parameter R , the probability p_0 of no interaction tends to zero, and the width of $p(\Delta E/\omega_c)$ broadens since a larger energy fraction ΔE is lost. In [10], an analytical approximation for $P(\epsilon)$ is given solely for illustrative purposes. It is based on the small- ω approximation $\frac{dI}{d\omega} \propto \alpha_s \sqrt{\frac{\omega_c}{\omega}}$ of an expression valid for large in-medium pathlengths only. We find that it captures well the shape of P for large systems where $p_0 \ll 1$. However it shows an unphysical large- ϵ tail with infinite first moment $\int d\epsilon \epsilon P(\epsilon)$. As seen from eq. (10) discussed below, the accuracy of our study profits significantly from a better numerical control of this large ϵ region.

The strong longitudinal and - to a lesser extent - transverse expansion of a heavy ion collision implies a decreasing density of scattering centers $n(\xi)$,

$$n(\xi)C = n_d C \left(\frac{\xi_0}{\xi} \right)^\alpha. \quad (7)$$

Here, $\alpha = 0$ characterizes a static medium and $\alpha = 1$ corresponds to a one-dimensional, boost-invariant longitudinal expansion consistent e.g. with hydrodynamical simulations. The maximal value n_d is reached around the formation time ξ_0 of the medium which can be set by the inverse of the saturation scale p_{sat} [16], resulting in $\approx 0.2 \text{ fm/c}$ at RHIC and $\approx 0.1 \text{ fm/c}$ at LHC. Since the difference between ξ_0 and the production time of the hard parton is irrelevant for the evaluation of the radiation spectrum (3), we replace the latter in (3) by ξ_0 .

We evaluate the gluon radiation spectrum for dynamically expanding collision regions over a wide range of expansion parameters $\alpha \in [0 : 1.5]$ by combining the

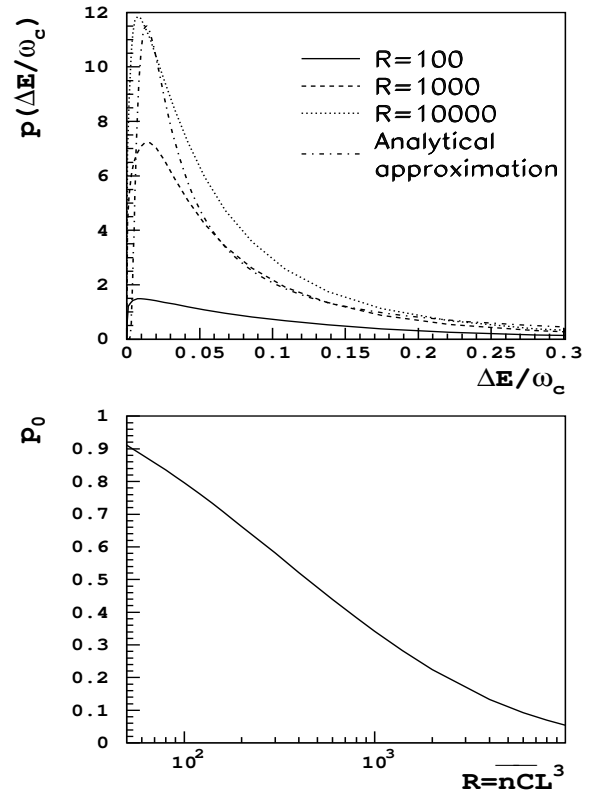


FIG. 1: The two contributions to the probability (2) that a parton loses ΔE of its energy in the medium: Continuous part (upper figure) and the discrete probability p_0 in (6) that the hard parton escapes the medium without interaction (lower figure).

analytic solution [6] of the path-integral (4) for a time-dependent harmonic oscillator with the treatment of finite size effects [11]. We observe a simple scaling law which relates the gluon radiation spectrum (3) of a dynamically expanding collision region to an equivalent static scenario. The linearly weighed line integral

$$\overline{nC} = \frac{2}{L^2} \int_{\xi_0}^{\xi_0+L} d\xi (\xi - \xi_0) n(\xi) C \quad (8)$$

defines the transport coefficient of the equivalent static scenario. Fig. 2 illustrates the accuracy of this scaling law for expansion parameters $\alpha = 0, 0.5, 1.0, 1.5$, and different values of the density parameter $R = \overline{nC}L^3$. The accuracy improved with increasing density parameter R . On the level of the quenching weight (2), it was better than 10 % in the physically relevant parameter range, except for very thin media ($R < 100$) where energy loss effects are negligible ($< 2\%$). In a subsequent publication [17], we shall extend this scaling law to the \mathbf{k}_\perp -differential radiation spectrum, and we shall document a CPU-inexpensive numerical routine which allows to implement the quenching weight (2) for arbitrary values of α , $n_d C$ and L in event generator studies of hadronic spectra.

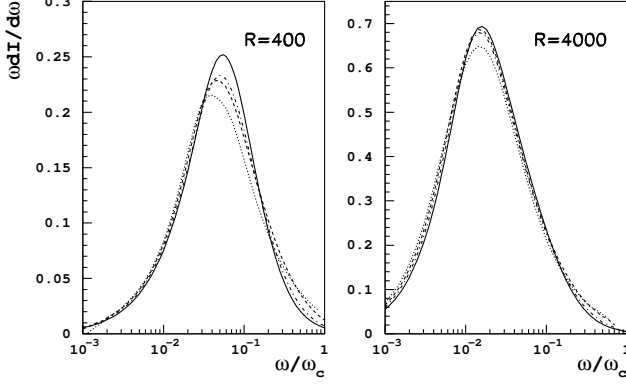


FIG. 2: The medium-induced gluon radiation spectrum $\omega \frac{dI}{d\omega}$ for different dynamical expansion parameters $\alpha=0$ (solid line), $\alpha=0.5$ (dotted-dashed), $\alpha=1$ (dashed) and $\alpha=1.5$ (dotted). The scaling law (8) is shown for $R=400$ and $R=4000$.

The linear weight in (8) implies that scattering centers which are further separated from the partonic production point ξ_0 are more effective in generating gluon radiation. For a dynamical expansion following Bjorken scaling [$\alpha = 1$ in eq. (7)], all timescales contribute equally to $\bar{n}\bar{C}$. This indicates that observables related to medium-induced gluon radiation give access to the quark-gluon plasma lifetime.

Since the radiation spectrum $\frac{dI}{d\omega}$ depends on the expansion parameter α , the length L and the transport coefficient only through $\bar{n}\bar{C}$, dynamical scaling holds automatically for the average parton energy loss

$$\langle \Delta E \rangle \equiv \int dE E P(E) = \int d\omega \omega \frac{dI}{d\omega}. \quad (9)$$

This is seen already from the expressions for $\langle \Delta E \rangle$ derived for dynamically expanding scenarios by Baier et al. [6] in the dipole approximation and by Gyulassy et al. [7] for $N = 1$ scattering center. Moreover, Gyulassy et al. [7] conjectured that higher order opacity terms ($N = 2, 3$) of $\langle \Delta E \rangle$ show the same dependence on $\bar{n}\bar{C}$. The results presented here go beyond establishing this conjecture and confirming the result of Ref. [6]. Our novel finding is that dynamical scaling holds beyond the ω -integrated average energy loss (9) to good numerical accuracy for the ω -differential gluon radiation spectrum. This is important since a reliable calculation of the medium-dependence of hadronic spectra requires [10] knowledge of the quenching weight (2) beyond the first moment (9) [i.e., requires knowledge about $\frac{dI}{d\omega}$]. Moreover, the scaling law established here is relevant for the angular gluon radiation pattern [17], since the radiation spectrum emitted outside the opening angle Θ can be calculated in the present approach essentially by replacing $R = n_0 C L^3 \rightarrow \sin^2 \Theta n_0 C L^3$.

We calculate the medium dependence of parton fragmentation functions $D_{h/q}(x, Q^2)$ from (1) using the quenching weights (2) and the LO BKK [15] parametrization of $D_{h/q}(x, Q^2)$. Typical results for the pion fragmentation function of up quarks are shown in Fig. 3. For the present study, we identify the virtuality Q of $D_{h/q}(x, Q^2)$ with the (transverse) initial energy E_q of the parton. This is justified since E_q and Q are of the same order, and $D_{h/q}(x, Q^2)$ has a weak logarithmic Q -dependence while medium-induced effects change as a function of $\epsilon = \frac{\Delta E}{Q} \approx O(\frac{1}{Q})$.

As seen in Fig. 3, the fragmentation function decreases for increasing values of the transport coefficient $\bar{n}\bar{C}$, since the probability of a parton of initial energy E_q to fragment into a hadron of large energy $x E_q$ decreases with increasing parton energy loss. The relative size of this medium modification changes roughly like $\epsilon = \frac{\Delta E}{Q} \approx O(\frac{1}{Q})$. We note that the calculation based on (1) is not reliable for small fractions x ($x < 0.1$ say), since it implies for $D_{h/q}^{(\text{med})}(x, Q^2)$ a normalization

$$\int_0^1 dx x D_{h/q}^{(\text{med})}(x) \simeq \int_0^1 dx x D_{h/q}(x) \int d\epsilon (1 - \epsilon) P(\epsilon), \quad (10)$$

which is a factor $\int d\epsilon \epsilon P(\epsilon)$ too small. The origin of this error is that the hadronized remnants of the medium-induced soft radiation are neglected in the definition of (1). Due to the softness of these remnants, however, the true medium modified fragmentation function is underestimated by equation (1) for small x only. We expect eq. (1) to be valid for the calculation of $D_{h/q}^{(\text{med})}(x, Q^2)$ for $x > 0.1$.

To illustrate the effect of medium-modified fragmentation functions on hadronic cross sections, we plot in Fig. 3 the fragmentation function multiplied by x^6 . This exploits that hadronic cross sections weigh the fragmentation function $D_{h/q}^{(\text{med})}(x, Q^2)$ by the initial hard partonic cross sections $d\sigma^q/dp_\perp^2 \sim 1/p_\perp^{n(\sqrt{s})}$ and thus effectively test $x^{n(\sqrt{s})} D_{h/q}^{(\text{med})}(x, Q^2)$. We choose $n = 6$ for illustrative purposes. For interpretation, the position of the maximum x_{max} of $x^6 D_{h/q}^{(\text{med})}(x, Q^2)$ corresponds to the most likely energy fraction $x_{\text{max}} E_q$ of the leading hadron. The medium-induced relative reduction of $x^6 D_{h/q}^{(\text{med})}(x, Q^2)$ around its maximum translates into a corresponding relative suppression of this contribution to the high- p_\perp hadronic spectrum at $p_\perp \sim x_{\text{max}} E_q$. For $Q = 10$ GeV, e.g., the leading hadron has most likely $p_\perp \sim 5 - 8$ GeV, and a reduction of this contribution to the pion spectrum by a factor 2 corresponds e.g. to $L = 7$ fm and $\bar{n}\bar{C} = 1 - 5 \text{ fm}^{-3}$, see Fig. 3. The transport coefficient can be related to the initial gluon rapidity density [2, 7]. Uncertainties in this procedure remain to be discussed. For the purpose of comparing our parameter values directly to results in the recent literature [7], we

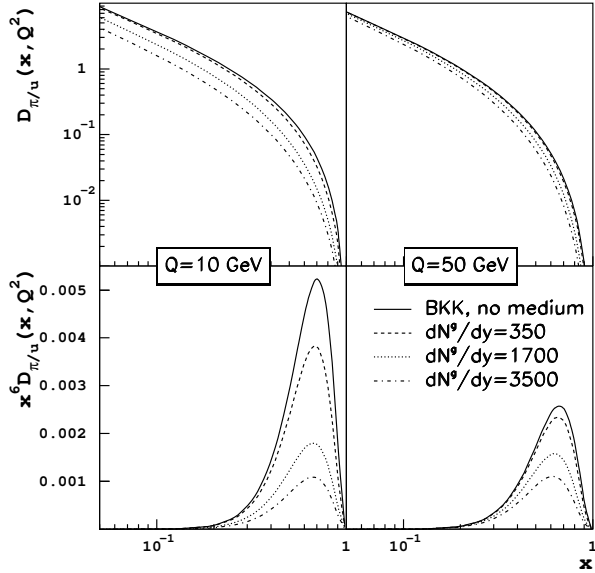


FIG. 3: The LO BKK [15] fragmentation function $u \rightarrow \pi$ for no medium and the medium-modified fragmentation functions for different gluon rapidity densities (see eq. (11)) and $L = 7$ fm.

use for a Bjorken scaling scenario

$$R = \overline{nC}L^3 = \frac{L^2}{R_A^2} \frac{dN^g}{dy}, \quad \text{for } \alpha = 1, \quad (11)$$

where R_A denotes the nuclear radius. The curves in Fig. 3 thus correspond to $\overline{nC} \approx 1, 5$ and 10 fm^{-3} , respectively.

A quantitative study of hadronic cross sections and a careful discussion of theoretical uncertainties is clearly needed for a detailed comparison of the above results to measured hadronic spectra. It is nevertheless interesting to contrast Fig. 3 with the transverse π^0 -spectrum measured at RHIC [18]. Taking the above-mentioned values at face value, the soft multiple scattering approach to parton fragmentation functions relates a medium-induced suppression factor ≈ 2 at $p_\perp \approx 5 \text{ GeV}$ to an initial gluon rapidity density which seems comparable with the value 500-1000 extracted in Ref. [7]. Thus, while the multiple soft BDMS scattering approach without finite size treatment was criticised [7] for overestimating the effects of parton energy loss below $p_\perp \approx 10 \text{ GeV}$ by up to an order of magnitude, the present findings and those obtained by a lowest order opacity expansion seem comparable. Differences pointed out [7] earlier do not allow to prefer the $N = 1$ opacity expansion over the multiple soft scattering approach but just indicate that finite size effects have to be treated in both approaches with the same scrutiny.

Equation (11) suggests that the average transport coefficient \overline{nC} changes from RHIC to LHC proportional to the observed particle multiplicity. Assuming a factor

~ 5 increase consistent with recent studies [16], Fig. 3 suggests the existence of a sweet spot at LHC energies in the p_\perp -range around 50 GeV, where theoretical uncertainties are much better controlled than at $p_\perp \leq 10 \text{ GeV}$ while suppression factors are still sufficiently large (of order 2) to be experimentally accessible. Attaching more precise numbers to this discussion lies beyond the exploratory calculation presented here. It does not only require a quantitative understanding of hadronic spectra in ultrarelativistic nucleus-nucleus collisions based on the knowledge of the underlying partonic cross sections and the nuclear parton distribution functions. It also requires medium-modified fragmentation functions for a realistic distribution of in-medium pathlengths L and initial densities. This in turn requires modeling of the spatio-temporal evolution of the hot and dense medium. The scaling law established here simplifies the inclusion of these dynamical effects in quantitative studies. It can be extended to the study of the medium-dependence of angular radiation patterns [17].

We thank F. Arleo, K. Eskola, A. Kovner, K. Redlich and V. Ruuskanen for helpful discussions. C.A.S. is supported by a Marie Curie Fellowship no. HPMF-CT-2000-01025 of the European Community TMR program.

-
- [1] M. Gyulassy and X. N. Wang, Nucl. Phys. B **420** (1994) 583.
 - [2] R. Baier, Y. L. Dokshitzer, A. H. Mueller, S. Peigne and D. Schiff, Nucl. Phys. B **484** (1997) 265.
 - [3] B. G. Zakharov, JETP Lett. **65** (1997) 615.
 - [4] U. A. Wiedemann, Nucl. Phys. B **588** (2000) 303.
 - [5] M. Gyulassy, P. Levai and I. Vitev, Nucl. Phys. B **594** (2001) 371.
 - [6] R. Baier, Y. L. Dokshitzer, A. H. Mueller and D. Schiff, Phys. Rev. C **58** (1998) 1706.
 - [7] M. Gyulassy, I. Vitev and X. N. Wang, Phys. Rev. Lett. **86** (2001) 2537.
 - [8] X. N. Wang, Z. Huang and I. Sarcevic, Phys. Rev. Lett. **77** (1996) 231.
 - [9] M. Gyulassy, P. Levai and I. Vitev, arXiv:nucl-th/0112071.
 - [10] R. Baier, Y. L. Dokshitzer, A. H. Mueller and D. Schiff, JHEP **0109** (2001) 033.
 - [11] U. A. Wiedemann, Nucl. Phys. A **690** (2001) 731.
 - [12] X. F. Guo and X. N. Wang, Phys. Rev. Lett. **85** (2000) 3591.
 - [13] J. W. Qiu and G. Sterman, arXiv:hep-ph/0111002.
 - [14] F. Arleo, talk at CERN TH workshop, 11-15 March 2002, <http://wwwth.cern.ch/lhcworkshop/lhcworkshop01.html> and arXiv:hep-ph/0201066.
 - [15] J. Binnewies, B. A. Kniehl and G. Kramer, Z. Phys. C **65** (1995) 471.
 - [16] K. J. Eskola, K. Kajantie, P. V. Ruuskanen and K. Tuominen, Nucl. Phys. B **570** (2000) 379.
 - [17] C.A. Salgado and U.A. Wiedemann, in preparation.
 - [18] G. David [PHENIX Collaboration], Nucl. Phys. A **698** (2002) 227.